

DEPOSITION OF SOLIDS FROM A PETROLEUM HEPTANE-SOLUBLE FRACTION UPON HEATING IN A MICRO-BOMB REACTOR

S. Venditti¹, C. Berruoco¹, P. Alvarez², T.J. Morgan¹, M. Millan^{*1}, A.A. Herod¹ and R. Kandiyoti¹

¹ Department of Chemical Engineering, Imperial College London, London SW7 2AZ, United Kingdom

² Instituto Nacional del Carbón, Consejo Superior de Investigaciones Científicas (CSIC), Oviedo, Spain

*Corresponding author: marcos.millan@imperial.ac.uk

ABSTRACT

Asphaltenes have been the subject of debate over the decades as they are generally considered to be the main cause of petroleum fouling. However, the experimental work described in this paper has provided some interesting and thought-provoking results. The asphaltene-free heptane-soluble (HS) fraction of a crude oil was heated up at high pressures in a batch micro-bomb reactor (MBR) for up to 24 hours. Experiments were carried out under conditions resembling those in pre-heat trains of refineries. Results showed deposit yields of up to 25 % of the original sample in weight.

Operating conditions – temperature in particular – were found to have a marked effect on the solubility properties of the products. Analysis of the liquid recovered from the MBR shows the formation of heptane insoluble material in the liquid crude in addition to deposits. This provides strong evidence of chemical changes occurring – even in the absence of shear stress related effects – as part of the fouling process. Molecular weight distributions and chemical structures have been examined by size exclusion chromatography and UV-fluorescence spectroscopy. This paper outlines an attempt at tracing the chemical changes taking place from feed to heat treated products, in terms of molecular masses and chemical structures.

A key finding of this work is that the contribution to fouling is not exclusive to asphaltenes, but that chemical reactions of different fractions, such as heptane soluble material, do play an important role in the mechanisms leading to deposit formation.

INTRODUCTION

Petroleum fouling has received much attention in recent years due to its economic and environmental consequences. Although our understanding of the problem has considerably improved, some aspects are still not well understood. It is generally assumed that deposition is related to the presence of asphaltenes, the heaviest and most polar fraction of crude oils. The contribution of other component parts of crude oils (e.g. resins) remains relatively unclear.

Predicting the phase behaviour of crude oils is always a difficult task, due on the one hand to the chemical complexity of crude oils, and, on the other, to the diversity of behaviour encountered between different crudes. The physical model of petroleum was simplified to four classes of materials (Wiehe et al., 2000), defined in terms of solubility separation according to a standard method: SARA

(Saturates-Aromatics-Resins-Asphaltenes). The largest and most aromatic materials (asphaltenes) are viewed as solids dispersed in the oil by resins, which are the second largest class in terms of aromatic group average sizes. According to this view, asphaltenes are kept dissolved in petroleum by a delicate balance which can be upset through the addition or removal of saturates/aromatics/resins and/or changes in temperature. According to Hong et al. (2004), the solubility of asphaltenes (heptane insoluble-toluene soluble fraction) in selected mixtures increases with the temperature over the 60 to 300°C range. However, thermo-chemical reactions occurring during the deposition process may change the solubility properties of crude oils. This area of study has not been adequately explored (Watkinson et al., 1997).

SARA results could be employed in estimating asphaltene stability in crude. Several methods have been proposed, one of them being based on the Asphaltene-Resin ratio (Asomaning, 2003). The application of this ratio has shown limitations in predicting asphaltene stability in some crudes. Subsequent works have shown Colloidal Instability Index as the best parameter to predict a crude oil's fouling propensity (Bennet et al., 2006), taking into account the influence of aromatics and saturates as well. In fact, contrary to lighter fractions, in which hydrocarbon structures are mainly aliphatic or monoaromatic, heavy fractions include naphthenic and aromatic structures with more than six alkylated cycles. Complex saturates and aromatic hydrocarbons can play a dominant role in the deposition mechanism (Merdrignac et al., 2007). However, how these molecular classes would interact in the absence/presence of asphaltenes, remains unclear.

The purpose of this study was to develop an alternative approach to understand the role that non-asphaltene crude oil components play in the deposition mechanism. The asphaltene-free heptane-soluble (HS) fraction of a crude oil was heated up at high pressures in a batch micro-bomb reactor. The main features of these experiments are uniform temperature profile and absence of flow stress. This configuration should allow the identification of the chemical transformations leading to deposit formation in a fashion independent from flow-related effects.

The products of heating up were then characterized. The analytical work was performed using SEC with a (6:1 v/v) NMP/CHCl₃ mixture as eluent, synchronous UV-fluorescence and ATR-infrared spectroscopy.

The work showed evidence of chemical reactions leading to deposition, which was more intense at higher temperatures. Chemical reactions appear to be the main

cause of shifts in oil composition, in terms of solubility classes. At that point the stability of the mixture will be determined by operating conditions and the final chemical composition. The fractionation of material deposited at 320°C showed the presence of heptane insoluble-toluene insoluble material (“coke”) and a heptane insoluble-toluene soluble phase (asphaltenes).

EXPERIMENTAL

Samples

Properties of the sample of crude oil (Crude B) used in the study are shown in Table 1.

Table 1: Crude oil properties.

| Parameter | Crude B |
|---------------------------------------|---------|
| API gravity | 24 |
| Viscosity (cst) @ 80 °C | 8.8 |
| Saturates (%wt.) | 22 |
| Aromatics (%wt.) | 66 |
| Resins (%wt.) | 6 |
| Asphaltene (% wt. in C ₇) | 7 |
| Colloidal Instability Index | 0.4 |
| S (% wt.) | 4 |
| Ni (ppm) | 25 |
| V (ppm) | 52 |

Crude oil fractionation

The separation of crude into heptane soluble (HS) and heptane insoluble (HI) fractions followed ASTM standard procedure (D3279-97).

Micro-bomb reactor experiments

3 ml of HS was heated up in a micro-bomb reactor (MBR), described in detail elsewhere (Zhang, 1996). The reactor was made of a ½ in bored-through Swagelok union tee and connected to the control head via a 1/4 in o.d. pressure line. The top of the pressure line was water-cooled by a small heat exchanger, serving to condense vapours and to protect the pressure transducer. A fluidised sand bath and a reactor shaker assembly were used for heating and stirring the reaction mixture respectively. The system is pressurised using N₂ which is inert chemically and reduces the autoxidation reactions. A set of runs was carried out, simulating conditions of industrial operation (Table 2). Run temperatures and residence times were varied in looking for possible contributions of the HS fraction in petroleum fouling.

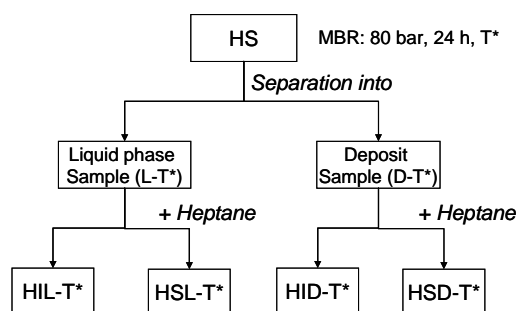


Figure 1: Schematic of MBR product recovery procedure.

Before product recovery, the reactor was externally cleaned, to ensure against product contamination. The vertical line was disconnected from the top and washed using CHCl₃ to collect the products. The reactor body was then detached from the vertical line, opened and emptied. The liquid phase (“L-T” - T denotes the temperature of the run.) was separated from the reactor and placed in a sample vial. Any deposits were then removed from the reactor wall using a spatula and weighed (D-T). A schema of the procedure and the following fractionation of the samples is shown in Figure 1.

Solubility test

Similar amounts (2 mg) of sample were mixed with the same volume of three different solvents (chloroform, NMP and toluene). The mixtures were shaken for about 1.5 hr after which the soluble and insoluble phases were separated after centrifugation. The soluble fractions were filtered, using a syringe filter with a pore diameter of 1 μm. Due to the behaviour of the insoluble material, which remains suspended in chloroform solution, vacuum filtration was used with a sinter Grade 4 (pore diameter between 5 and 15 μ). Both fractions were dried and weighed, and the solubility was calculated from the following equation:

$$S = \frac{B - I}{B} \times 100 \quad (1)$$

where B is the weight of the initial sample and I is the weight of the insoluble material. To avoid contamination with NMP-oxidation products that might form during the drying process, soluble and insoluble fractions of this solvent were dried under a N₂ flow and gentle heating (Berruoco et al, 2009). The procedure was repeated three times and the standard deviation estimated with a maximum value of 5% for these samples.

Size exclusion chromatography (SEC)

A 30 cm long, 7.5 mm o.d. column, packed with 5 μm polystyrene-divinylbenzene polymer particles (‘Mixed-D’ column, Polymer Laboratories Ltd, UK) was operated at 80 °C at an eluent flow rate of 0.50 ml min⁻¹. The solvent was a solution of NMP/CHCl₃ (ratio 6:1). Detection was carried out using a Perkin-Elmer LC290 variable wavelength UV absorbance detector. Calibration with polystyrene (PS) and polyaromatic hydrocarbon standards (PAHs) and operating conditions have been previously described in detail (Berruoco et al. 2008).

UV-fluorescence (UV-F)

The procedure has been described elsewhere (Morgan et al. 2005). The Perkin-Elmer LS51 luminescence spectrometer was set with a slit width of 25 nm, to scan at 240 nm min⁻¹; synchronous spectra were acquired at a constant wavelength difference of 20 nm. A quartz cell with 1 cm path length was used. The spectrometer featured automatic correction for changes in source intensity as a function of wavelength. Emission, excitation and synchronous spectra of the sample were obtained in

NMP/CHCl₃ 6:1 v/v ratio for all the samples; only synchronous spectra are shown. Finally, the spectra were height normalized to facilitate the comparison.

ATR-IR

All the FTIR spectra were measured using a Spectrum 100 FTIR spectrometer (PerkinElmer) with a Pike Miracle detector. The solid samples were deposited on a modified attenuated total reflection (ATR) accessory (ZnSe crystal). Spectra were obtained with a spectral resolution of 2 cm⁻¹ and 8 scans in the 4000-800 cm⁻¹ wavenumber range. Spectra were corrected from scattering using 'Baseline' (Software version 6.2.0.0055). From the obtained spectra, the aromaticity index was calculated according to the equation (Guillen et al. 1992) using the relative intensities of the signals:

$$I_{ar} = \frac{Abs_{3050}}{Abs_{3050} + Abs_{2920}} \quad (2)$$

where Abs₃₀₅₀ corresponds to the aromatic C-H stretching modes between 3100 and 3000 cm⁻¹, and Abs₂₉₂₀ is the aliphatic C-H stretching modes between 3000 and 2700 cm⁻¹.

RESULTS

Characterisation of liquid phase samples

Table 2 shows the weight percentage of deposits obtained from micro-bomb reactor runs in relation with their operating conditions and feed material.

Table 2: Micro-bomb reactor experiments run for 24 hours at 80 bars.

| N° Run | Feed Processed | T (°C) | D (%wt.) |
|--------|----------------|--------|----------|
| Run 1 | HS Crude B | 390 | 26 |
| Run 2 | HS Crude B | 320 | 10 |
| Run 3 | HS Crude B | 280 | n.d. |
| Run 4 | Crude B | 390 | 19 |
| Run 5 | Crude B | 320 | 1 |
| Run 6 | Crude B | 280 | n.d. |

n.d. no deposits

The amount of deposits increased with temperature. More recent results (not shown in this paper) suggest an increase in the amount of deposits with the residence time as well as changes in the chemical composition and structure (aging effect). A clear effect of feed material on the results could be observed. Furthermore, the percentage of deposits obtained from the heptane-soluble runs was higher than those obtained using the whole crude, for similar operating conditions. As it has been commented before, the resin-asphaltene interaction is thought to play an important role in the stability of the crude (Leon et al, 2000). Modifications in the resin/asphaltene ratio may affect the stability and explains the higher amount of deposits obtained in Runs 1-3 in comparison with Runs 4-6.

Figure 2 presents size exclusion chromatograms of the liquid phase samples obtained from the MBR experiments, allowing for a comparison between retention times of the main eluted peaks and the corresponding temperature

values. Two features in the figure are relevant. First, the chromatogram of the liquid phase sample corresponding to the run at highest temperature (L-390) shows a retained peak shifted to longer elution times (smaller masses) in comparison with the feed material (Crude B HS), suggesting the presence of lighter material in this fraction (250 u in according with the PAH calibration, Berruoco et al, 2008). Secondly, there are slight differences between the runs at lower temperature, with larger molecules in L-280. As no deposits have been obtained at 280 °C, most of the heavy products appear to have remained in the liquid phase. This may explain why L-320 was lighter than L-280 (10 % deposits obtained at 320 °C).

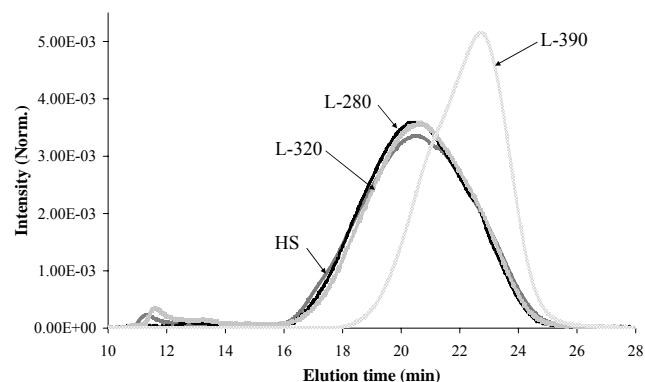


Figure 2: Area normalized SEC chromatograms of HS, L-280, L-320 and L-390.

The UV-fluorescence technique is used to compare aromatic ring systems (chromophores). As the polynuclear aromatic groups become larger, their UV-F spectrum shifts towards longer wavelengths. This information can be indirectly related to the molecular size. Another feature is that the ability to fluoresce varies with the MW of the sample and decreases when the size increases (Li et al., 1994; Strausz et al., 2002). In Figure 3, the synchronous UV-F spectra of the heated samples were all shifted to shorter wavelengths compared to the spectrum of the HS-sample. The significance of small variations in the spectra of L-280 and L-320 is unclear.

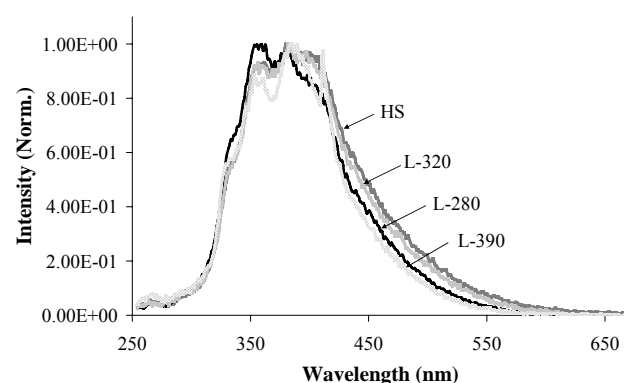


Figure 3: Synchronous UV-F spectra of HS, L-280, L-320 and L-390

A clear overall trend toward shorter wavelengths may, nevertheless, be observed between the spectra of the HS sample and the liquid phase heated to the highest temperature, L-390.

The characterisation of liquid samples does not show significant differences between the runs especially at low temperature. This fact led to the use of different solvents to fractionate the sample in order to make the identification easier via the isolation of different classes of compounds. All the samples have been separated into heptane-soluble and heptane-insoluble fractions. Results are shown in Figure 4. Thus, starting with a heptane-soluble fraction, results from heating to all three temperatures has led to the formation of heptane-insoluble material, although no deposits were recovered at L-280.

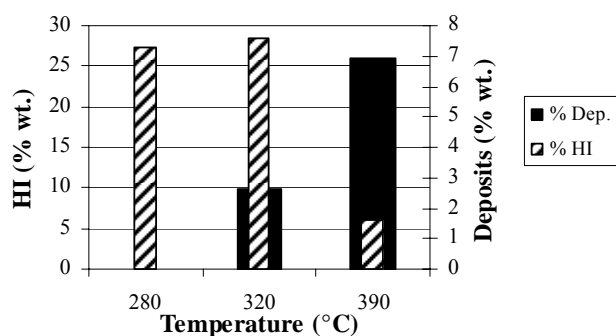


Figure 4: Comparison between HI recovered from liquids and deposits

The observed changes in the solubility class of significant amounts of material strongly suggests that chemical reactions are taking place within these samples, even at the lowest test temperature (i.e. 280 °C). The changes observed during characterization, i.e., decrease in solubility, increase in molecular weight, and increase of aromatic group size, are all consistent with a polymerization mechanism leading to carbonization and coking of the sample (Lewis, 1980, 1982). The carbonization mechanism also includes thermal cracking reactions, which are more relevant at temperatures above 350 °C.

Table 3: Elution time and mass estimates from SEC of heat exchanger deposits

| Sample | Retained Peak Max. | | | |
|---------|--------------------|----------|--------------------------|-----------------------|
| | Time / mins | Mass / u | Δt^1 Time / mins | Δm^2 Mass / u |
| L-280 | 20.6 | 250 | | |
| HIL-280 | 18.5 | 450 | 2.0 | 200 |
| L-320 | 20.7 | 250 | | |
| HIL-320 | 19.4 | 350 | 1.3 | 100 |
| L-390 | 22.8 | 150 | | |
| HIL-390 | 20.3 | 300 | 2.5 | 150 |

¹ $\Delta t = (\text{elution time L-X}) - (\text{elution time HIL-X})$
² $\Delta m = (\text{molecular mass L-X}) - (\text{molecular mass HIL-X})$

Overall, Figure 4 shows decreasing proportions of HI-material in the liquid phase, as the amount of precipitated deposit increased with temperature. All HI fractions (“HIL”) have been characterised by SEC and UV-Fluorescence spectroscopy; results are summarized in Table 3.

The maximum intensity of the peak of material resolved by column porosity was found to have shifted by about 2.5 minutes, which corresponds to a difference of about 100-200 u between the liquid and its HI fraction, as calculated using the PAHs calibration (Berruenco et al, 2008).

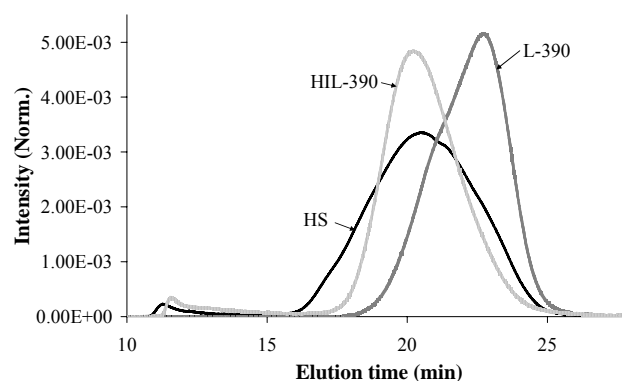


Figure 5: Area normalized SEC chromatograms of L-390 and HIL-390

Figure 5 presents size-exclusion chromatograms of the HIL-390 and L-390 samples. As expected, there was a shift to shorter elution times (greater masses) between the L-390 (liquid phase) to the HI fraction, signalling the presence of larger molecules in the HI-sample. The corresponding UV-F results (Figure 6) show a shift towards longer wavelengths for the HI fraction compared to the liquid. This indicates that the biggest polynuclear aromatic systems are present in the HI-fraction. This is consistent with the larger molecular mass material present in this fraction, as observed by SEC.

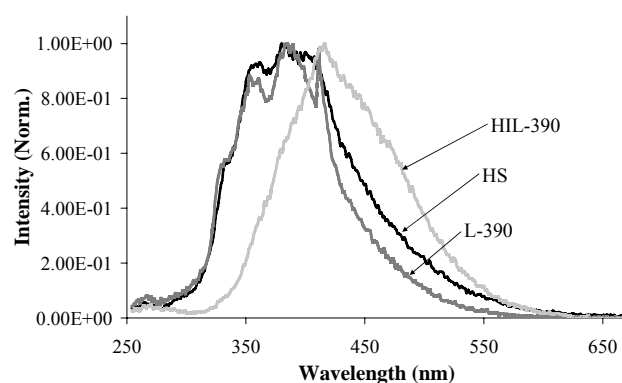


Figure 6: Synchronous UV-F spectra of L-390 and HIL-390

Figure 7 shows the variation between SEC chromatograms of the HI fractions, as a function of temperature. At 280 °C the HI fraction shows the larger molecules followed by those at 320 °C and 390 °C.

Figure 8 presents synchronous UV-fluorescence spectra of the same three fractions, all shifted to longer wavelengths compared to the “liquid” phases, suggesting the presence of larger aromatic chromophores in the HIL-samples.

It is relevant to observe that Crude B Asphaltenes have similar molecular mass distribution compared to HIL-280

and slightly larger size of chromophores than those of HI recovered from low temperature runs.

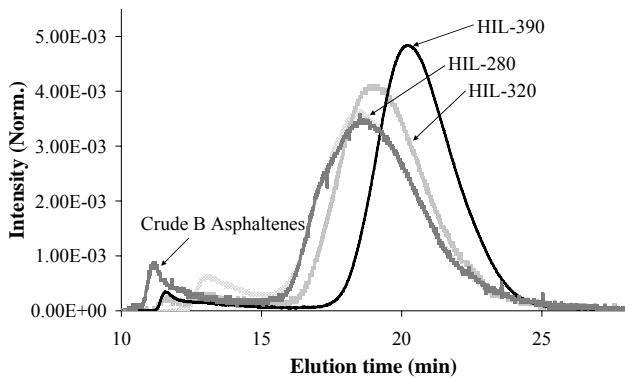


Figure 7: Area normalized SEC chromatograms of liquid HI fractions in comparison with Crude B asphaltenes.

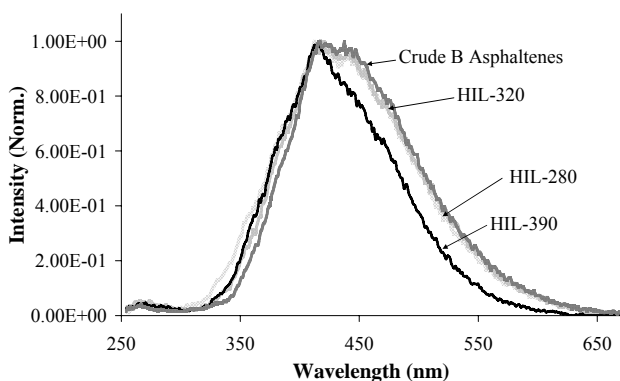


Figure 8: Synchronous UV-F spectra of liquid HI fractions in comparison with Crude B asphaltenes.

Characterisation of deposit samples

The characterisation of deposits is key to understand fouling mechanisms. Due to the complexity of the samples and the limitations of individual analytical techniques, a combination of several of them is required to characterise deposited foulants. The approach developed in this work consists of the use of several complementary techniques, in order to glean information about molecular mass distributions, chemical structures and compositions. As a first step, a solubility test has been performed, to evaluate the behaviour of the deposits in solution. Results are shown in Table 4. Standard deviation has been estimated from ± 0.6 to ± 5.0 %.

Table 4: Solubility test results

| Solvent | Solubility (%) | |
|--------------------------------|----------------|--------------|
| | D-390 | D-320 |
| Chloroform | 56 \pm 5.0 | 90 \pm 4.9 |
| 1-methyl-2-pyrrolidinone (NMP) | 46 \pm 2.1 | 75 \pm 1.7 |
| NMP/CHCl ₃ (6:1) | 51 \pm 4.0 | 89 \pm 2.3 |
| Heptane | 27 \pm 0.6 | 67 \pm 0.9 |
| Toluene | 42 \pm 1.2 | 73 \pm 1.3 |

Because most of petroleum-derived species are largely soluble in chloroform and toluene, these two solvents have

been employed to conduct this test. In addition, NMP and heptane have been utilized in order to have a better understanding of the organic species in the first case and the percentage of heptane-insoluble fraction produced from these runs in the second case. Solubility in the mixture NMP/CHCl₃ (6:1) has been finally estimated due to the use of this eluent in the SEC system. It is worth noting that only the soluble fraction of the samples will be analysed by this technique.

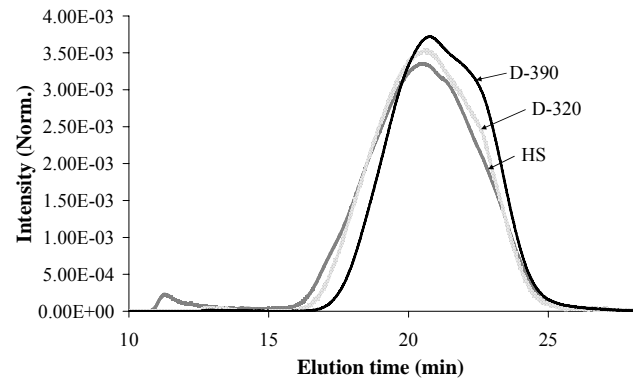


Figure 9: Area normalized SEC chromatograms of D-320 and D-390 in comparison with HI.

The results show that the best solvents are chloroform and NMP, in that order. The solubility of the deposits decreased with increasing run temperature.

Size exclusion chromatograms of D-320 and D-390 are shown in Figure 9. The two samples showed significantly different solubility in the mixture used as eluent (89 % and 51 % respectively). The sample recovered at the higher temperature (D-390) has smaller molecular weight compared to that at lower temperature (D-320). However, synchronous UV-F spectra (Figure 10) indicate larger chromophores present in D-390 and smaller ones in D-320 in comparison with HS.

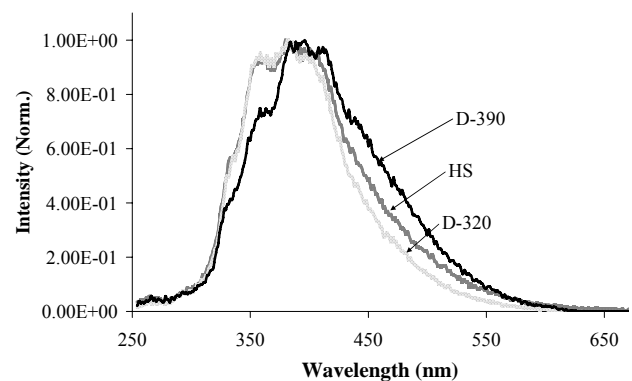


Figure 10: Synchronous UV-F spectra of D-320 and D-390 in comparison with HI.

The ATR-IR spectra of liquid samples are shown in Figure 11. The results showed that no bands in the 3900 to 3100 cm⁻¹ region, indicating low concentrations of OH or NH groups. Peaks in the range of 3000 to 2800 cm⁻¹ are related to the aromaticity index by equation (2) (Table 5). The results indicate that the MBR products exhibited higher proportions of aromatic hydrogen (higher aromaticity

index) than the feed material and that the aromaticity of the samples increased, in general, with the temperature.

Table 5: Aromaticity index of the samples (ATR-IR spectra)

| | HS | L-280 | L-320 | L-390 | D-320 | D-390 |
|----------|------|-------|-------|-------|-------|-------|
| I_{ar} | 0.19 | 0.20 | 0.20 | 0.25 | 0.17 | 0.20 |

In the 1750-1600 cm^{-1} region, only the D-390 sample showed a peak at 1700 cm^{-1} corresponding to carboxylic acids. In addition, D-390, D-320 and L-390 showed a peak at 1600 cm^{-1} , which is related to the C=C aromatic double bond being more abundant in D-390. The 1600 cm^{-1} band is known as the coke band and shifted to a lower wavelength for longer aged deposit (Fan and Watkinson, 2006). These results indicate that the aged deposits have a more typical condensed polyaromatic structure.

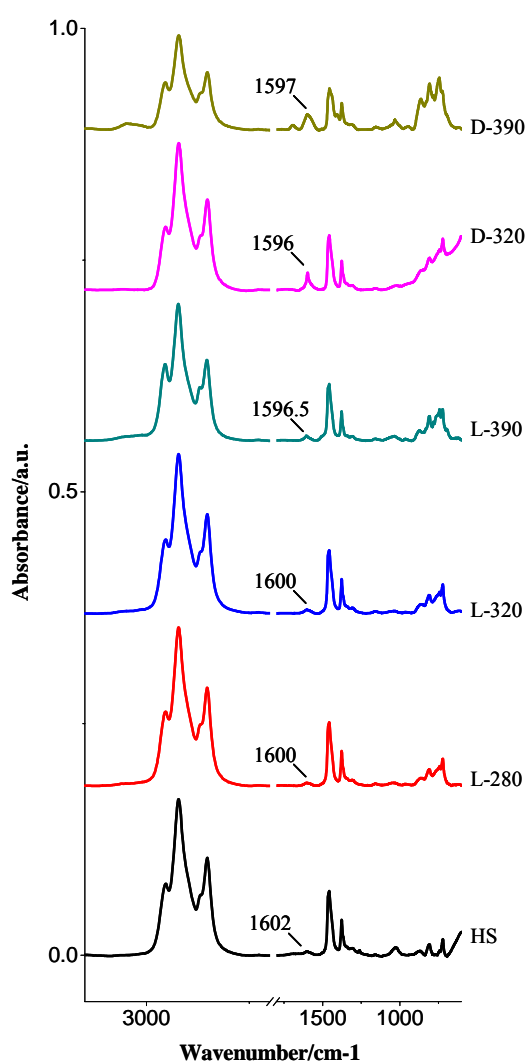


Figure 11: ATR-IR of the liquid phase and deposit samples.

The band assignment in the 1300-1500 cm^{-1} region is CH_3 and CH_2 alkyl chains bending mode with more intense signal for HS.

It is noticeable that the C=S assignment (1026 cm^{-1}) is present for D-390; aliphatic sulphides are the most

thermally reactive functionality and can react to form FeS, which could explain the high sulphur content in the deposits, as has been demonstrated previously (Srinivasan, 2005). Finally, the 900-700 cm^{-1} region showed the aromatic out-of-plane vibration of aromatic C-H bonds. Three main peaks are observed in all the spectra with different intensity. The band at about 865 cm^{-1} corresponds to isolated aromatic hydrogen. The band in the range 850-800 cm^{-1} may be attributed to systems containing two and/or three adjacent hydrogens. The peak at 750 cm^{-1} is due to the ortho-substitution of the aromatic rings (Guillen et al., 1992).

A further fractionation of one of the deposits (that from Run 5) has been performed and a schematic of this procedure is shown in Figure 12.

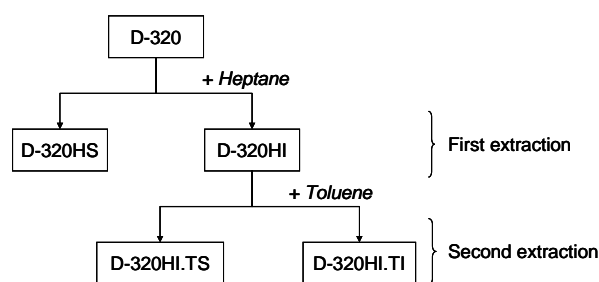


Figure 12: Schematic of D-320 fractionation.

The deposit from Run 5 has been chosen for this purpose because it was obtained at a relatively low temperature (320°C), more closely resembling that of an industrial heat exchanger. D-320 has been separated into heptane soluble and insoluble fractions (66 % and 32 % respectively in the first extraction). The formation of heptane-insolubles from heptane-soluble feed material appears to point to mild polymerization of the sample. In a second extraction, the heptane insoluble fraction has been fractionated into toluene soluble and insoluble fraction. The mass balance data is summarized in Table 6.

Table 6: Mass balance of D-320 fractionation

| Sample | Notation | % of deposit | % of D-320HI |
|---|-------------|--------------|--------------|
| Deposit from Run 5 | D-320 | 100.0 | n/a |
| Heptane insoluble fraction of the deposit (first extraction) | D-320HI | 33 | 100 |
| Heptane soluble fraction of the deposit (first extraction) | D-320HS | 66 | n/a |
| Toluene soluble fraction of the heptane insoluble (second extraction) | D-320 HI.TS | 4 | 12 |
| Toluene insoluble fraction of the heptane insoluble (second extraction) | D-320 HI.TI | 29 | 88 |

During Run 5, 10 % of the sample was observed to form deposits. 4 % of D-320 was heptane insoluble-toluene soluble (definition of asphaltene) and 29 % was both heptane and toluene insoluble (“coke”). The high proportion of coke formed appears related to the thermochemical reactions occurring during the run. It is known that the extent of conversion of asphaltenes into “coke” is affected by temperature and ageing (Rahmani et al, 2002). These results clearly show that it is possible to precipitate deposits from an asphaltene-free sample at relatively low temperatures.

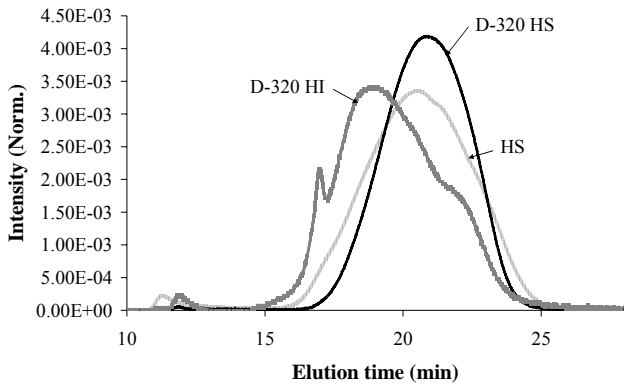


Figure 13: Area normalized SEC chromatograms of D-320HI and D-320HS

All sub-fractions have been characterized by SEC and UVF. Figure 13 shows the size-exclusion chromatograms of the products of the first extraction. The maximum intensity of the retained peak was found to have shifted by about 2 minutes, from 20.9 minutes (D-320HS) to 18.9 minutes (D-320HI), which corresponds to molecular masses of 250 and 770 respectively as calculated using the PS and the PAH calibrations (Berruoco et al. 2008).

The retained peak lift-off at the high mass end from D-320 HI, HS, D-320 HS appears at 14.8, 15.8 and 16.6 min, respectively. These elution times correspond to PS masses of 20,000 u, 9,000 u and 5,000 u, in the same order.

Figure 14 shows Synchronous UV-F spectra of the same three samples.

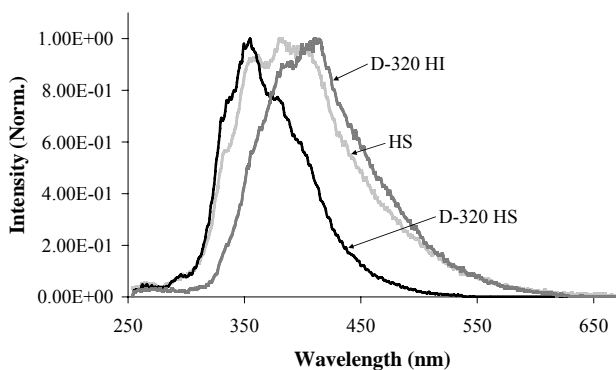


Figure 14: Synchronous UV-F spectra of D-320HI and D-320HS

The spectra show a shift towards shorter wavelengths from D-320HI to D-320HS (smaller aromatic chromophores); this seems to be in agreement with the SEC

conclusions. Both techniques suggest the presence of larger aromatic clusters in the D-320 HI fraction.

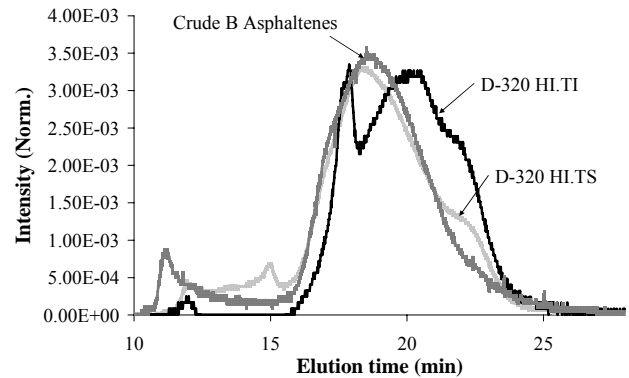


Figure 15: Area normalized SEC chromatograms of D-320HI.TI and D-320HI.TS

Figure 15 shows the size-exclusion chromatograms of the products of the second extraction. In what follows, TI denotes toluene insoluble material and TS denotes toluene soluble material. D-320 HI.TI and D-320 HI.TS are compared with Crude B Asphaltenes. We recall that D-320 HI.TI and D-320 HI.TS have different solubilities in the eluent mixture used (with lower solubility for D-320 HI.TI). In Figure 15, the maximum intensity of the retained peak was found to have shifted by about 2 minutes, from 20.4 minutes (D-320HI.TI) to 18.4 minutes (D-320HI.TS), which correspond to molecular masses of 300 u and 1100 u respectively as calculated using the PS and the PAH calibrations. This suggests the presence of larger molecules in D-320HI.TS.

Another important finding is related to the comparison between Crude B Asphaltenes and D-320HI.TS, which are the asphaltenes generated during the experiment. The maximum intensity of the retained peak is 18.7 minutes for Crude B Asphaltenes and 18.4 minutes for D-320HI.TS, which corresponds to 1100 u and 900 u respectively (PS calibration). More information can be gleaned by looking at the UV-F results (Figure 16). D-320HI.TI synchronous spectrum indicates the presence of larger aromatic chromophores than D-320 HI.TS. In addition, the results show a shift towards longer wavelengths from D-320 HI.TS to Crude B Asphaltenes.

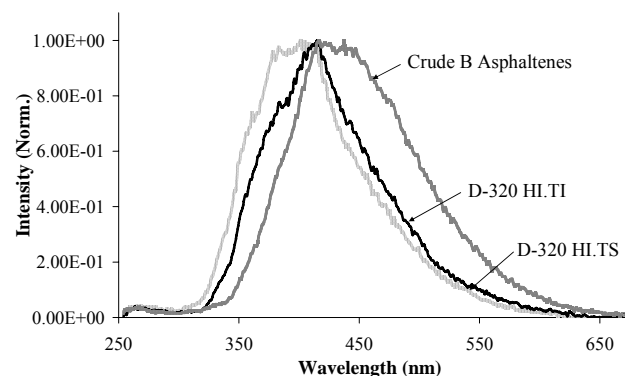


Figure 16: Synchronous UV-F spectra of D-320HI.TI and D-320HI.TS

The comparison between D-320 HITS and Crude B Asphaltenes shows similarities in terms of molecular weight but significant differences regarding the size of polynuclear aromatic cores.

CONCLUSIONS

Asphaltenes are generally considered as the main cause of petroleum fouling. However, in this work, deposited foulants have been obtained from a fraction of crude oil that did not contain asphaltene. The asphaltene-free heptane-soluble (HS) fraction of a crude oil was heated up at high pressures in a batch micro-bomb reactor. The results from runs with heptane soluble as feed material have shown solubility changes in the sample with formation of heptane insolubles (HI) in samples heated to 280, 320 and 390 °C, for 24 hrs. Deposit precipitation out of solution was observed at the two higher temperatures, 320°C and 390°C.

The study shows that the amount of deposit increases with rising temperature, and also depends on the chemical composition of the original crude oil. The proportion of deposits obtained from heating the heptane-soluble fraction was greater than those obtained using the whole crude (Crude B) at the same operating conditions.

Several analytical techniques have been used to examine the chemical/structural properties of deposits obtained in the micro bomb reactor (MBR). The results, in terms of solubilities, molecular mass (SEC), structure (UV-F) and functionalities (ATR-IR) reflect that the deposition process is intimately linked to chemical reactions (ageing and coking processes), which become more intense at higher temperatures. These indications were also confirmed with the fractionation of the deposits obtained at 320°C from heptane soluble (D-320). The formation of different solubility fractions, in particular the heptanes-insoluble-toluene insoluble subfraction, and the changes observed in molecular masses and structures provides evidence of chemical reactions.

This work shows that the contribution to fouling is not exclusive to asphaltene, but that chemical reactions of different fractions, such as heptane soluble material, could play an important role in the mechanisms leading to deposit formation.

NOMENCLATURE

Iar aromaticity index, dimensionless

REFERENCES

Asomaning, S., 2003, Test Methods for determining Asphaltene Stability in Crude Oils, *Petroleum Science and Technology*, Vol. 21, pp. 581-590.

Bennet, C. A., Appleyard, S., Gough, M., Hohmann, R. P., Joshi, H. M., King, D. C., Lam, T. Y., Rudy, T. M. and Stomierowski, S. E., 2006, Industry-Recommended Procedures for Experimental Crude Oil Preheat Fouling Research, *Heat Transfer Engineering*, Vol. 27(9), pp.28-35.

Berruoco, C., Alvarez, P., Venditti, S., Morgan, T. J., Herod, A. A., Millan-Agorio, M. and Kandiyoti, R., 2009, Sample Contamination with NMP-oxidation Products and

By product-free NMP Removal from Sample Solution, *Energy & Fuels*, Vol. 23, pp. 3008-3015.

Berruoco, C., Venditti, S., Morgan, T.J., Alvarez, P., Millan-Agorio, M., Herod, A.A., Kandiyoti, R., 2008, Calibration of Size-Exclusion Chromatography Column with 1-Methyl-2-pyrrolidinone (NMP)/Chloroform mixture as eluent: applications to petroleum-derived samples, *Energy & Fuels*, Vol. 22, pp. 3265-3274.

Fan, Z. and Watkinson, 2006, Aging of carbonaceous deposits from heavy hydrocarbon vapors, *Ind. Eng. Chem. Res.*, Vol. 45, pp. 6104-6110.

Fan, Z. and Watkinson, 2006, Formation and characteristic of carbonaceous deposits from heavy hydrocarbon coking vapors, *Ind. Eng. Chem. Res.*, Vol. 45, pp. 6104-6110.

Guillen, M. D., Iglesias M. J., Dominguez, A. and Blanco, C. G., 1992, Semiquantitative FTIR analysis of a coal tar pitch and its extracts and residues in several organic solvents, *Energy & Fuels*, Vol. 6, pp. 518-525.

Hong, H. and Watkinson, P., 2004, A study of asphaltene solubility and precipitation, *Fuel*, Vol. 83, pp. 1881-1887.

León, O., Rogel, E., Espidel, J. And Torres, J., 2000, Asphaltene: Structural Characterization, Self-Association, and Stability Behavior *Energy & Fuels*, 14, pp. 6-10.

Lewis, I. C., 1980, Thermal Polymerization of aromatic hydrocarbons, *Carbon*, Vol. 18, pp. 191-196.

Lewis, I. C., 1982, Chemistry of carbonization, *Carbon*, Vol. 20, pp. 519-259.

Li, C-Z., Wu, F., Cai, H-Y. and Kandiyoti, R., UV-Fluorescence of coal pyrolysis tars, 1994, *Energy and Fuels*, 1994, Vol. 8, pp. 1039-1048.

Merdrignac, I. and Espinat, D., 2007, Physicochemical Characterisation of Petroleum Fractions: the State of the Art, *Oil & Gas Science and Technology*, Vol. 26, pp. 7-32.

Morgan, T. J., Millan, M., Behrouzi, M., Herod, A. A. and Kandiyoti, R., 2005, On the limitations of UV-fluorescence spectroscopy in the detection of high-mass hydrocarbon molecules, *Energy & Fuels*, Vol. 19, pp. 164-169.

Rahmani, S., McCaffrey, W. and Gray, M.R., 2002, Kinetics of Solvent Interaction with Asphaltene during coke formation, *Energy&Fuels*, Vol. 16, pp. 148-154.

Srinivasan, M. and Watkinson, P., 2005, Fouling of Some Canadian Crude Oils, *Heat Transfer Engineering*, Vol. 26, pp. 7-14.

Strausz, O., Peng, P. and Murgich, J., 2002, About the colloidal nature of asphaltene and the MW of covalent monomeric units, *Energy & Fuel*, Vol. 16, pp. 809-822.

Watkinson, P. and Wilson, I., 1997, Chemical Reaction fouling: a review, *Experimental Thermal and Fluid Science Inc.*, Vol. 14, pp. 361-374.

Wiehe, I. and Kennedy, R. J., 2000, The Oil Compatibility Model and Crude Oil Incompatibility, *Energy & Fuels*, Vol. 14, pp. 56-59.

Zhang, S., Xu, B., Herod, A.A. and Kandiyoti, R., 1996, Hydrocracking reactivities of primary coal extracts prepared in a flowing-solvent reactor, *Energy & Fuels*, 10, 733-742.